Physics of Plasmas

Resonance broadening effect for relativistic electron interaction with electromagnetic ion cyclotron waves

Cite as: Phys. Plasmas **29**, 082903 (2022); https://doi.org/10.1063/5.0101792
Submitted: 03 June 2022 • Accepted: 29 July 2022 • Published Online: 23 August 2022

D. S. Tonoian, A. V. Artemyev, X.-J. Zhang, et al.

Physics of Plasmas ARTICLE scitation.org/journal/php

Resonance broadening effect for relativistic electron interaction with electromagnetic ion cyclotron waves

Cite as: Phys. Plasmas **29**, 082903 (2022); doi: 10.1063/5.0101792
Submitted: 3 June 2022 · Accepted: 29 July 2022 ·
Published Online: 23 August 2022

View Online Export Citation CrossMark

D. S. Tonoian,[1,2,a)] A. V. Artemyev,[1,3] X.-J. Zhang,[3] M. M. Shevelev,[1] and D. L. Vainchtein[1,4]

AFFILIATIONS

[1]Space Research Institute of the Russian Academy of Sciences (IKI), Moscow 117997, Russia
[2]Faculty of Physics, National Research University Higher School of Economics, Moscow 105066, Russia
[3]Institute of Geophysics and Planetary Physics, University of California, Los Angeles, California 90095, USA
[4]Nyheim Plasma Institute, Drexel University, Camden, New Jersey 08103, USA

[a)]Author to whom correspondence should be addressed: tonoian.ds17@gmail.com

ABSTRACT

Relativistic electron scattering by electromagnetic ion cyclotron (EMIC) waves is one of the most effective mechanisms for >1 MeV electron flux depletion in the Earth's radiation belts. Resonant electron interaction with EMIC waves is traditionally described by quasi-linear diffusion equations, although spacecraft observations often report EMIC waves with intensities sufficiently large to trigger nonlinear resonant interaction with electrons. An important consequence of such nonlinear interaction is the resonance broadening effect due to high wave amplitudes. In this study, we quantify this resonance broadening effect in electron pitch-angle diffusion rates. We show that resonance broadening can significantly increase the pitch-angle range of EMIC-scattered electrons. This increase is especially important for ∼1 MeV electrons, where, without the resonance broadening, only those near the loss cone (with low fluxes) can resonate with EMIC waves.

I. INTRODUCTION

Relativistic electron scattering by electromagnetic ion cyclotron (EMIC) waves is one of the most effective mechanisms for electron losses in the Earth's radiation belts.[12,14,23,52,60,62] For typical EMIC wave characteristics (see discussion on the definition of such typical characteristics in Ref. 69), the resonant electron energies are above ∼1 MeV for field-aligned electrons (see Refs. 19, 43, 58, and 70), and even higher for higher pitch-angles (the angle between electron velocity and background magnetic field). Such an increase in the resonant energy with pitch-angle implies that EMIC waves cannot scatter the main population of relativistic electrons (at ∼1–3 MeV), which are highly anisotropic with maximum fluxes at ∼90° pitch-angles (see discussions in Refs. 34, 40, and 44). Therefore, the overall contribution of EMIC waves to the net losses of relativistic electrons (i.e., the so-called electron dropouts[29,48]) still requires additional investigations, although their scattering rates can be very large.[34,43,60,70]

Several mechanisms have been proposed to extend the energy/pitch-angle range of electrons that can be explained by EMIC wave scattering. First, the cold plasma dispersion of EMIC waves suggests a higher wave number around the frequency cutoff of hydrogen, helium, and oxygen gyrofrequencies,[43,57] and, thus, the high-frequency fraction of EMIC spectrum may effectively scatter electrons at moderate pitch-angles.[9,20,61] However, such high-frequency EMIC waves are rarely observed and do not contribute significantly to the main wave statistics.[34,67] Second, hot plasma effects in the EMIC wave dispersion relation may potentially extend the pitch-angle range of scattered electrons.[9,42,53] For most of observed EMIC waves, however, such hot plasma effects tend to increase the minimum resonant energy[17,19] and, thus, decrease the resonant pitch-angle range. Third, whistler-mode waves may contribute to electron scattering from high pitch-angles to pitch-angles resonating with EMIC waves,[40,68] but this mechanism would require the simultaneous presence of both wave modes (EMIC and whistlers) along the electron drift path.[68] Fourth, very intense EMIC waves can resonate with electrons nonlinearly,[2,26,45,46] and the phase trapping by field-aligned[55] or oblique[63] intense EMIC waves may transport electrons into loss cone from a wider pitch-angle range than as expected from the quasi-linear model. Fifth, the resonant pitch-angle range can be extended by the effect of the resonance width.[4,31] The variant of this effect driven by a large wave amplitude has been examined for whistler-mode waves[15] but not yet quantified for EMIC waves. Here, we focus on the fourth mechanism and provide theoretical descriptions of how it alters electron scattering by EMIC waves.

The finite resonance width effect (also known as the resonance broadening) is most important for large-amplitude waves, with the particle momentum resonant range proportional to the square root of wave amplitude.[32,50] As EMIC waves can be very intense with wave amplitudes reaching a few percent of the background magnetic field,[24,30,67] the finite resonance effect may significantly expand the pitch-angle range of scattered electrons. To illustrate this effect, we analyze relativistic electron pitch-angle distributions collected during an intense EMIC wave event.[11] Figure 1(a) shows electron fluxes vs pitch-angle α, with the flux normalized to values at $\alpha \sim 90^\circ$. For all energies, there is a clear flux decrease toward the loss-cone (small α) and anti-loss-cone ($\alpha \sim 180^\circ$), and such a flux gradient is likely formed due to electron scattering by simultaneously observed EMIC waves. However, the estimated range of resonant pitch-angles (estimated from the cold plasma dispersion using observed wave characteristics) is much narrower than the pitch-angle range with the flux gradient [see dashed curves in panel (a)]. Therefore, additional mechanisms are needed to explain the observed flux gradients over an expanded pitch-angle range. We then include the finite resonance width into the calculation of resonant electron pitch-angles in Fig. 1(b). This effect significantly expands the pitch-angle range: dashed lines cover almost the entire pitch-angle range exhibiting a flux gradient. Although Fig. 1 demonstrates the potential importance of the finite resonance width effect, this event is mostly for illustration purpose. In this study, we theoretically quantify the resonance broadening effect and show how to include it in EMIC wave diffusion rate calculations, which have been widely used in radiation belt models. However, it still needs further validation from a systematic comparison of EMIC-driven electron pitch-angle distributions from observations and from theoretical predictions, which is left for future studies. Such a multi-event comparison will also help reveal contributions from alternative mechanisms in shaping the observed electron pitch-angle distributions (e.g., even for the event in Fig. 1, an additional scattering mechanism, in addition to EMIC waves, is likely operating to cause the flux depletion around 90°, as resonances with EMIC waves cannot create such flux minima).

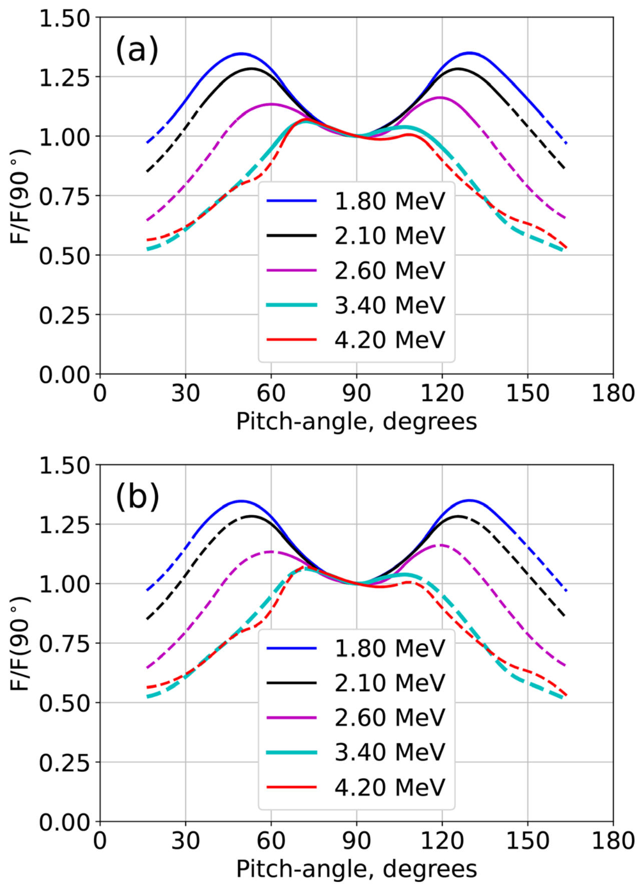

FIG. 1. Pitch-angle distributions of relativistic electrons observed during an EMIC wave event on 2017-02-16 06:47-06:52 UT. Distributions are collected by the relativistic electron proton telescope,[8] averaged over the EMIC wave interval, and normalized to fluxes at 90° pitch-angle. EMIC wave and background field characteristics for this interval are wave intensity $B_w^2 \approx 1.053$ nT^2, wave mean frequency $f/f_{cp} = 0.187$, plasma frequency to gyrofrequency ration $f_{pe}/f_{ce} = 31.25$, with 20% of helium and 10% of oxygen (see details in Ref. 11). Solid lines show observed distributions, whereas dashed lines show the pitch-angle range corresponding to resonant interactions with observed EMIC waves without (a) and with (b) the resonance broadening effect included.

This paper is organized as follows: Sec. II provides the theoretical framework of evaluating the finite resonance width effect for electrons resonating with EMIC waves in the inhomogeneous magnetic field; Sec. III describes how this effect can be incorporated into the diffusion rate evaluation; Sec. IV discusses the obtained results.

II. BASIC EQUATIONS FOR WAVE-PARTICLE RESONANCE IN INHOMOGENEOUS MAGNETIC FIELD

We start our quantification of the resonance broadening effect with the Hamiltonian of a relativistic electron (the rest mass is m_e and charge is $-e$) moving in the electromagnetic field given by the vector potential $\mathbf{A} = (A_x, A_0 + A_y, 0)$:

$$H = \sqrt{m_e^2 c^4 + c^2 p_z^2 + (cp_x + eA_x)^2 + (eA_0 + eA_y)^2}, \tag{1}$$

where (z, p_z) are the conjugate pair of the field-aligned coordinate and momentum, (x, p_x) are the conjugate pair of the transverse coordinate and momentum, and $A_0(x, z) = xB_0(z/R)$ is the vector potential component of the curvature-free dipole field[10] with the spatial scale $R \gg m_e c^2/eB_0$. For the background magnetic field B_0, we use $B_0 = B_{eq}\sqrt{1 + 3\sin^2\lambda}/\cos^6\lambda$, with B_{eq} is the equatorial magnetic field and λ is the magnetic latitude. The relation between z and λ is given by the differential equation $dz/d\lambda = R\sqrt{1 + 3\sin^2\lambda}\cos\lambda$, with $R = R_E L$, L is the L-shell parameter, and R_E is the Earth radius. Vector potential components for L-mode field-aligned plane waves, $A_{x,y}(z, t)$, are given by the following equation:

$$A_{x,y} = \frac{B_w}{k}\begin{cases} -\cos\phi, & \partial\phi/\partial z = k, \\ \sin\phi, & \partial\phi/\partial t = -\omega. \end{cases} \tag{2}$$

Wave amplitude B_w is sufficiently small, so that $eB_w/km_e c^2 \ll 1$. For a fixed wave frequency ω, the wave number k is given by the cold plasma dispersion relation,[54]

$$\left(\frac{kc}{\omega}\right)^2 = 1 - \frac{\omega_{pe}^2}{\omega(\omega+\Omega_{ce})} - \sum_{i=1}^{3}\frac{\omega_{pi}^2}{\omega(\omega-\Omega_{ci})}, \tag{3}$$

where $\Omega_{ce} = eB/m_e c$, ω_{pe} is the plasma frequency, and indexes $i = 1$, 2, and 3 are attributed to H^+, He^+, and O^+ ions, respectively.

We substitute wave vector potential components to Hamiltonian (1) and introduce the magnetic moment I_x as

$$p_x = m_e c\sqrt{\frac{2I_x\Omega_{ce}}{m_e c^2}}\sin\theta, \quad x = \frac{c}{\Omega_{ce}}\sqrt{\frac{2I_x\Omega_{ce}}{m_e c^2}}\cos\theta$$

and expand Hamiltonian over the small wave energy $eB_w/km_ec^2 \ll 1$ to get[1,3]

$$\begin{aligned} H &\approx m_e c^2\gamma + \sqrt{\frac{2I_x\Omega_{ce}}{m_e c^2}}\frac{eB_w}{k\gamma}\sin(\phi-\theta), \\ \gamma &= \sqrt{1+\left(\frac{p_z}{m_e c}\right)^2 + \frac{2I_x\Omega_{ce}(z)}{m_e c^2}}, \end{aligned} \tag{4}$$

where (θ, I_x) are conjugate variables of gyrophase and magnetic moment

$$\dot\theta = \frac{\partial H}{\partial I_x} = \frac{\Omega_{ce}}{\gamma}.$$

The resonance condition for Hamiltonian (4) can be written as

$$\dot\phi - \dot\theta = -\frac{\Omega_{ce}}{\gamma} + k\frac{p_z}{m_e\gamma} - \omega = 0. \tag{5}$$

This is the first cyclotron resonance of relativistic electrons and field-aligned EMIC waves. To estimate the range of resonant p_z, i.e., the finite resonance width, we shall follow the approach proposed in Refs. 7, 41, and 51 and examine Hamiltonian (4) around the resonance. First, let us introduce $\psi = \phi - \theta$ as a new Hamiltonian variable conjugate to the momentum I. For this reason, we use the generating function $W(\theta, z; I, p; t) = (\phi-\theta)I + pz$ with new variables,

$$\begin{aligned} \psi &= \frac{\partial W}{\partial I} = \phi - \theta, \quad I_x = \frac{\partial W}{\partial \theta} = -I, \\ s &= \frac{\partial W}{\partial p} = z, \quad p_z = \frac{\partial W}{\partial z} = kI + p. \end{aligned} \tag{6}$$

A new Hamiltonian $\mathcal{H} = H + \partial W/\partial t$ has the following form:

$$\begin{aligned} \mathcal{H} &= m_e c^2\gamma - \omega I + \sqrt{\frac{-2I\Omega_{ce}}{m_e c^2}}\frac{eB_w}{k\gamma}\sin\psi, \\ \gamma &= \sqrt{1+\left(\frac{p+kI}{m_e c}\right)^2 - \frac{2I\Omega_{ce}}{m_e c^2}} \end{aligned} \tag{7}$$

with conjugate variables (s, p) and (ψ, I). Note that introducing ψ leads to a new $\tilde I_x$ constant because $\mathcal{H}$ does not depend on θ. Thus, we set $\tilde I_x = 0$, i.e., $I = -I_x$ at the initial moment (note I does not change in the absence of waves).

The resonance condition in new Hamiltonian variables is

$$\dot\psi = -\frac{\Omega_{ce}}{\gamma} + k\frac{p+kI}{m_e\gamma} - \omega = 0. \tag{8}$$

This condition determines the resonant $I = I_R(s, p)$

$$I_R = -\frac{p}{k} + \frac{m_e\Omega_{ce}}{k^2} + \frac{m_e\omega}{k^2}\frac{1}{\sqrt{1-(\omega/kc)^2)}}\sqrt{1+2\frac{p}{mc}\frac{\Omega_{ce}}{kc} - \frac{\Omega_{ce}^2}{(kc)^2}}. \tag{9}$$

Substituting I_R to the Lorentz factor (7), we obtain the following resonant energy:

$$\gamma_R = \frac{1}{\sqrt{1-(\omega/kc)^2}}\sqrt{1+2\frac{p}{mc}\frac{\Omega_{ce}}{kc} - \frac{\Omega_{ce}^2}{(kc)^2}}. \tag{10}$$

Hence, the resonance momentum can be written as

$$I_R = -\frac{p}{k} + \frac{m_e\Omega_{ce}}{k^2} + \frac{m_e\omega}{k^2}\gamma_R. \tag{11}$$

Expansion of Hamiltonian near the resonance gives

$$\mathcal{H} \approx m_e c^2\gamma_R - \omega I_R + \frac{1}{2}K^2(I_x - I_R)^2 + \sqrt{-\frac{2I_R\Omega_{ce}}{m_e c^2}}\frac{eB_w}{k\gamma_R}\sin\psi, \tag{12}$$

where

$$K^2 = m_e c^2\frac{\partial^2\gamma}{\partial I^2}\bigg|_{I=I_R} = \frac{k^2c^2-\omega^2}{\gamma_R m_e c^2}.$$

Then, we use the generating function $F(\psi, s; P_\psi, \tilde p; t) = (P_\psi + I_R(s, p(\tilde p, s)))\psi + \tilde p s$ to introduce a new variable momentum $P_\psi = I - I_R$,

$$\begin{aligned} \tilde\psi &= \frac{\partial F}{\partial P_\psi} = \psi, \quad I = \frac{\partial F}{\partial \psi} = P_\psi + I_R, \\ \tilde s &= \frac{\partial F}{\partial \tilde p} = s + \frac{\partial I_R}{\partial \tilde p}\psi, \quad p = \frac{\partial F}{\partial s} = \tilde p + \frac{\partial I_R}{\partial s}\psi. \end{aligned} \tag{13}$$

The smallness of the second terms in expressions of new variables $(\tilde s, \tilde p)$ allows us to expand the Lorentz term $m_e c^2\gamma_R - \omega I_R$ as follows:

$$\begin{aligned} & m_e c^2\gamma_R(s,p) - \omega I_R(s,p) \\ &\approx m_e c^2\gamma_R(\tilde s,\tilde p) - \omega I_R(\tilde s,\tilde p) \\ &\quad - m_e c^2\left(\frac{\partial\gamma_R}{\partial s}\frac{\partial I_R}{\partial\tilde p}\psi + \frac{\partial\gamma_R}{\partial p}\frac{\partial I_R}{\partial s}\psi\right) \\ &\approx m_e c^2\gamma_R(\tilde s,\tilde p) - \omega I_R(\tilde s,\tilde p) + m_e c^2\{I_R, \gamma_R\}\psi. \end{aligned}$$

New Hamiltonian

$$\tilde{\mathcal{H}} \approx m_e c^2\gamma_R - \omega I_R + \frac{1}{2}K^2P_\psi^2 + A\psi + B\sin\psi \tag{14}$$

can be separated into two parts $\tilde{\mathcal{H}} = \Lambda + \mathcal{H}_\Psi$: $\Lambda = m_e c^2\gamma_R - \omega I_R$ describes the slow particle motion in the (s, p) plane and

$$\mathcal{H}_\psi = \frac{1}{2}K^2P_\psi^2 + A\psi + B\sin\psi \tag{15}$$

describes fast particle oscillations around the resonance.[3,7,41,51] Coefficients of $\mathcal{H}_\psi$ depend on (s, p) and change along electron trajectories,

$$B = \sqrt{\frac{2I_R\Omega_{ce}}{m_e c^2}\frac{eB_w}{k\gamma_R}}$$

and

$$\begin{aligned}\frac{A}{m_e c^2} = \{I_R, \gamma_R\} &= \frac{\partial I_R}{\partial s}\frac{\partial \gamma_R}{\partial p} - \frac{\partial \gamma_R}{\partial s}\frac{\partial I_R}{\partial p}\\ &= -\frac{\partial \ln \Omega_{ce}}{\partial s}\frac{1}{k\gamma_R}\frac{1}{1-(\omega/kc)^2}\\ &\quad\times\left\{\frac{p_R}{m_e c}\frac{\Omega_{ce}}{kc} + \frac{kI_R}{m_e c}\frac{\Omega_{ce}}{kc} + \frac{\partial \ln k}{\partial \ln \Omega_{ce}}\left(\frac{p_R}{m_e c}\right)^2\right\},\end{aligned}$$

where $p_R = m_e(\omega\gamma_R + \Omega_{ce})/k$.

Hamiltonian $\mathcal{H}$ does not depend on time, and, thus, any change of I should correspond to change of energy: $m_e c^2 \Delta\gamma = \omega \Delta I$. From equations of motion

$$\begin{aligned}\Delta I = -\int_{-\infty}^{+\infty}\frac{\partial \mathcal{H}}{\partial \psi}dt &= -2\int_{-\infty}^{\psi_*}\frac{\partial \mathcal{H}}{\partial \psi}\frac{\partial t}{\partial \psi}d\psi\\ &= -\sqrt{\frac{2}{K^2}}\int_{-\infty}^{\psi_*}\frac{B\cos\psi\, d\psi}{\sqrt{\mathcal{H}_\psi - A\psi - B\sin\psi}},\end{aligned} \tag{16}$$

where $\psi_* = \psi_*(\mathcal{H}_\psi)$ is the phase value at the resonance for a given $\mathcal{H}_\psi$ (see Fig. 2). Function $\Delta I(\mathcal{H}_\psi)$ is periodic with a period of 2π. The width of the resonance is $\Delta I(\mathcal{H}_\psi)$ averaged over H_ψ,

$$\langle \Delta I\rangle = -\frac{1}{2\pi}\frac{\sqrt{2}}{K}\int_0^{2\pi} dh \int_{-\infty}^{\psi_*}\frac{B\cos\psi\, d\psi}{\sqrt{h - A\psi - B\sin\psi}}. \tag{17}$$

This expression can be written as[7]

$$\langle \Delta I\rangle = \frac{1}{\pi}\sqrt{\frac{2B}{K^2}}f\left(\frac{A}{B}\right), \tag{18}$$

where $f(A/B)$ is the area surrounded by the separatrix

$$f = \int_{\psi_X}^{\psi_{\max}} d\psi \sqrt{\frac{A}{B}(\psi_X - \psi) + (\sin\psi_X - \sin\psi)}. \tag{19}$$

The integration limits, ψ_X and ψ_{max}, are shown in Fig. 2. Profile of the $f(A/B)$ function and analytical fitting of this function are shown in Fig. 3. Note that $\psi_X = \arccos(A/B)$ and for $A/B \to 0$, we have $f = \int_0^{2\pi} d\psi\sqrt{1-\sin\psi} = 4\sqrt{2}$.

The resonance width in terms of ΔI can be rewritten to the resonance width in energy

$$m_e c^2\langle\Delta\gamma\rangle = \frac{\omega}{\pi}\sqrt{\frac{2B}{K^2}}f\left(\frac{A}{B}\right) \tag{20}$$

and in pitch-angle

$$\begin{aligned}\langle\Delta\alpha_{eq}\rangle &= \arcsin\sqrt{\sin^2\alpha_{eq} + \frac{\Omega_{ce,eq}}{\omega}\frac{2\langle\Delta\gamma\rangle}{(\gamma^2-1)}} - \alpha_{eq}\\ &\approx \frac{2\langle\Delta\gamma\rangle}{(\gamma^2-1)\sin(2\alpha_{eq})}\frac{\Omega_{ce,eq}}{\omega},\end{aligned} \tag{21}$$

where α_{eq} and $m_e c^2(\gamma - 1)$ are the initial equatorial pitch-angle and energy.

Combining Eqs. (18), (20), and (21) with the fitting of f function (see Fig. 3), we plot the resonant pitch-angle width for several typical wave characteristics. Figure 4 shows that $\Delta\alpha_{eq}$ maximizes at low energies, where the effect of the resonance broadening should be most important because of the narrow pitch-angle range of electrons satisfying the exact resonant condition with EMIC waves [see Fig. 1(a)]. The resonance width $\Delta\alpha_{eq}$ can reach 25°, which will allow EMIC waves to scatter the main (trapped) electron population well outside the pitch-angle range of quasi-linear diffusion rates.[22,23,40,43] Note that the resonance width in energy, $\Delta\gamma$, is proportional to the wave frequency ω, i.e., for static magnetic field perturbations with $\omega = 0$, there is no energy change at the resonance and the resonance width $\Delta\gamma \to 0$ with

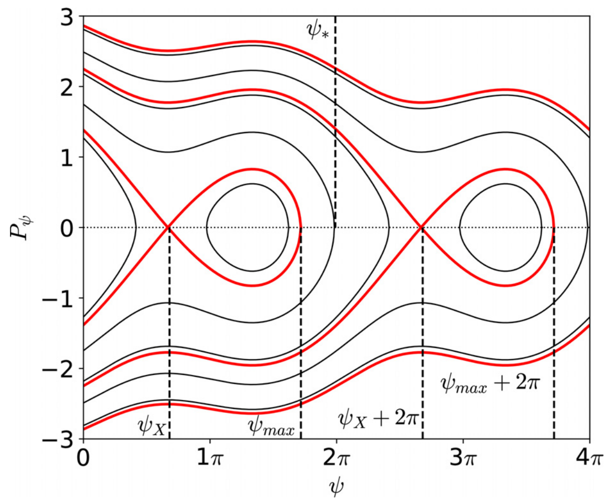

FIG. 2. Phase portrait for Hamiltonian $\mathcal{H}_\psi$ in the (ψ, P_ψ) plane.

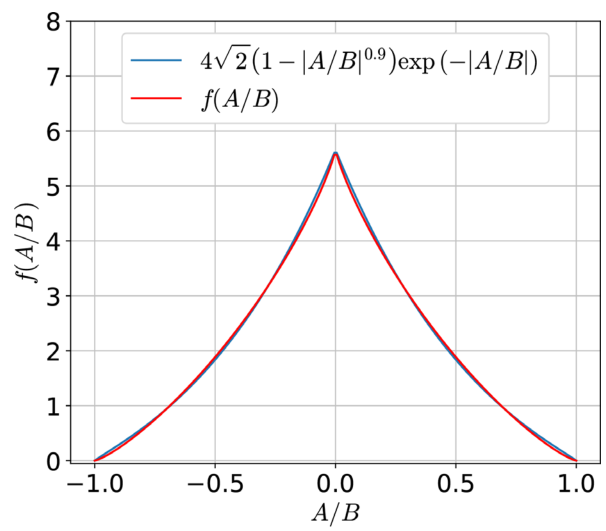

FIG. 3. Function $f(A/B)$ and its analytical fitting of $f = 4\sqrt{2}(1 - |A/B|^{0.9})\exp(-|A/B|)$.

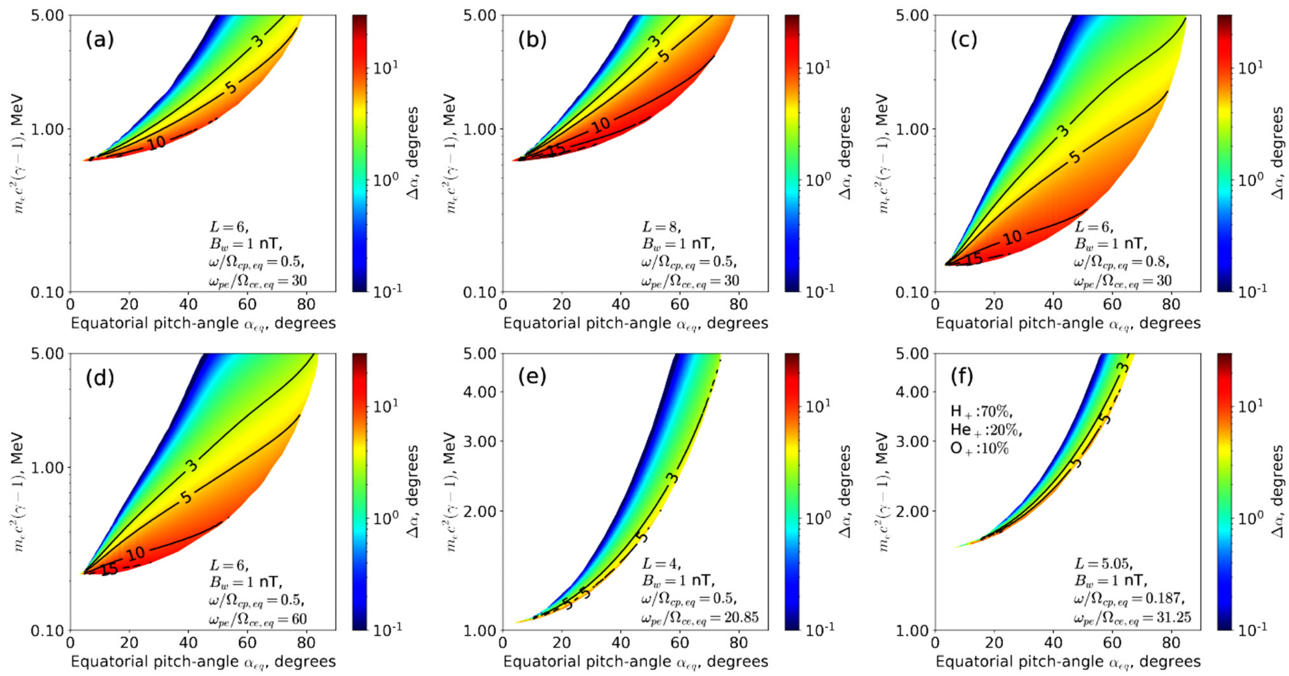

FIG. 4. The resonance width in equatorial pitch-angles as a function of $\alpha_{eq}, m_e c^2(\gamma - 1)$ for different wave frequencies and L-shells. (a)–(d) The case of electron-proton plasma; (e) the case for parameters from Fig. 5; parameters for case (f) are from Fig. 1.

a finite $\Delta\alpha_{eq}$, see discussions in Ref. 65. Therefore, for EMIC waves with $\omega/\Omega_{ce,eq} \ll 1$, the energy change $\Delta\gamma$ (and the resonance width) is negligibly small.[2,45]

III. ROLE OF RESONANCE BROADENING IN ELECTRON PITCH-ANGLE DIFFUSION

Determining the resonance width as a function of wave characteristics, electron energy, and pitch-angle, we can include the resonance broadening effect into diffusion rate calculations. We start with the local (at equator) pitch-angle diffusion for field-aligned EMIC waves with truncated Gaussian spectra ($\tilde{W}(\omega) \propto \exp\{-[\omega - \omega_m]^2/\delta\omega^2\}$) propagating in a proton-electron plasma,[58]

$$D_{\alpha\alpha} = \frac{\Omega_{ce}}{\gamma} \cdot \frac{2R}{\nu\delta x} \int_{x_1}^{x_2} \mathrm{d}x \left(g(x - x_r) \frac{x(1-x)}{(2-x)} \mathrm{e}^{-[(x-x_m)/\delta x]^2} \right), \quad (22)$$

where $x = \omega/\Omega_{ci}$, Ω_{ci} is the proton gyrofrequency, x_1 and x_2 are lower and upper cutoff frequencies, x_r is the normalized resonance frequency for a given equatorial electron pitch-angle and energy, $R = (B_w/B_0)^2$ is the normalized wave intensity, and $\nu = \sqrt{\pi}\mathrm{erf}(1) \approx 1.49$. In the classical formulation of the quasi-linear diffusion rate,[33] function $g = \delta(x - x_r)$ is the Dirac delta function. In Refs. 15 and 31, the finite resonance width can be included into the diffusion rate evaluations by changing g to

$$g(x) = \begin{cases} (2\Delta x)^{-1}, & |x| < \Delta x, \\ 0, & |x| \geq \Delta x, \end{cases} \quad (23)$$

where the resonance width in frequency is determined from the local resonance condition,

$$\Delta x = \frac{k}{\partial k/\partial x} \cdot \left[-\frac{\gamma}{\gamma^2 - 1}\Delta\gamma + \tan\alpha\Delta\alpha \right].$$

Figure 5(a) shows local (equatorial) diffusion rates with $g = \delta(x - x_r)$ (solid lines) and with g given by Eq. (23) (dashed lines). The resonance broadening effect is most clearly seen as an extension of the pitch-angle range with a finite diffusion rate.

Equations (18), (20), and (21) determine the resonance width at the resonant latitude for a given energy and equatorial pitch-angle. Therefore, $\Delta\alpha_{eq}$ and Δx vary with latitudes, and we can incorporate the resonance broadening effect into the bounce-averaged diffusion rate,[38]

$$\langle D_{\alpha_{eq}\alpha_{eq}} \rangle = \frac{1}{\tau} \int_0^{\lambda_m} D_{\alpha\alpha} \frac{\cos\alpha}{\cos^2\alpha_{eq}} \cos^7\lambda \mathrm{d}\lambda, \quad (24)$$

where $D_{\alpha\alpha} = D_{\alpha\alpha}(\gamma, \alpha_{eq}, \lambda)$, and we use the dipole magnetic field model with $\sin^2\alpha = \sin^2\alpha_{eq}\sqrt{1 + 3\sin^2\lambda}/\cos^6\lambda$. The normalized bounce period is $\tau \approx 1.3 - 0.56\sin\alpha_{eq}$ (see, e.g., Ref. 49).

Figure 5(b) shows bounce averaged diffusion rates without (solid curves) and with (dashed curves) the resonance broadening effect. There is a clear extension of the resonance pitch-angle range to higher pitch-angles due to the finite $\Delta\alpha$. This effect should be most important for low resonant energies, where the exact resonant condition only allows scattering of near loss-cone electrons.

IV. DISCUSSION AND CONCLUSIONS

In this study, we quantify the resonance broadening effect for EMIC waves resonating with relativistic electrons. The basic idea of the

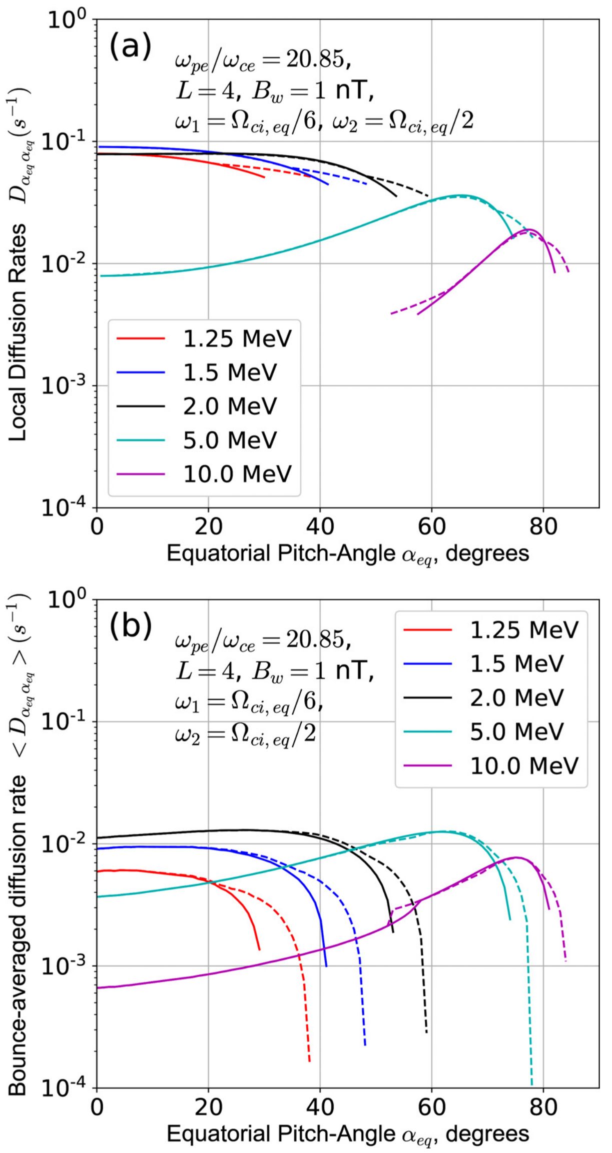

FIG. 5. Local (equatorial) (a) and bounce-averaged (b) diffusion rates without (solid) and with (dashed) the resonance broadening effect included. Wave and background system parameters are taken from the diffusion rate calculation example in Ref. 56.

resonance broadening involves the effect of charged particle motion in resonance with waves of a finite amplitude B_w/B_0 (see Refs. 32, 47, and 50). Although the perturbation theory requires B_w/B_0 to be small, the resonance width $\sim\sqrt{B_w/B_0}$ may provide an important widening of the resonant energy, pitch-angle ranges for specific plasma populations. The best example is the resonance broadening for whistler-mode waves resonating with large pitch-angle electrons, where the finite resonance width allows scattering of nominally non-resonant equatorial electrons.[15,16] Energies of electrons resonating with EMIC waves are generally higher than 1 MeV, and for lower resonant energies, only field-aligned electrons can be scattered.[34,43] However, fluxes of these relativistic electrons are strongly anisotropic, with the main population at higher pitch-angles, not reachable for the exact resonance with EMIC waves.[22,34,40,68] The resonance broadening effect extends the pitch-angle range of scattered electrons and allows EMIC wave to contribute to losses of the main electron population. It is worth noting that our results have been obtained for field-aligned EMIC waves but may be generalized to oblique waves using the same Hamiltonian approach.[1,7] The main difference for oblique waves will be the presence of multiple cyclotron resonances, including Landau resonance, which is particularly important for equatorial electrons.[63]

An important characteristic controlling the efficiency of the resonance broadening is the ratio of background magnetic field gradient and wave intensity, i.e., ratio A/B in Fig. 3. For cases with $|A/B| < 1$, the wave intensity is sufficiently high to create a finite resonance width,

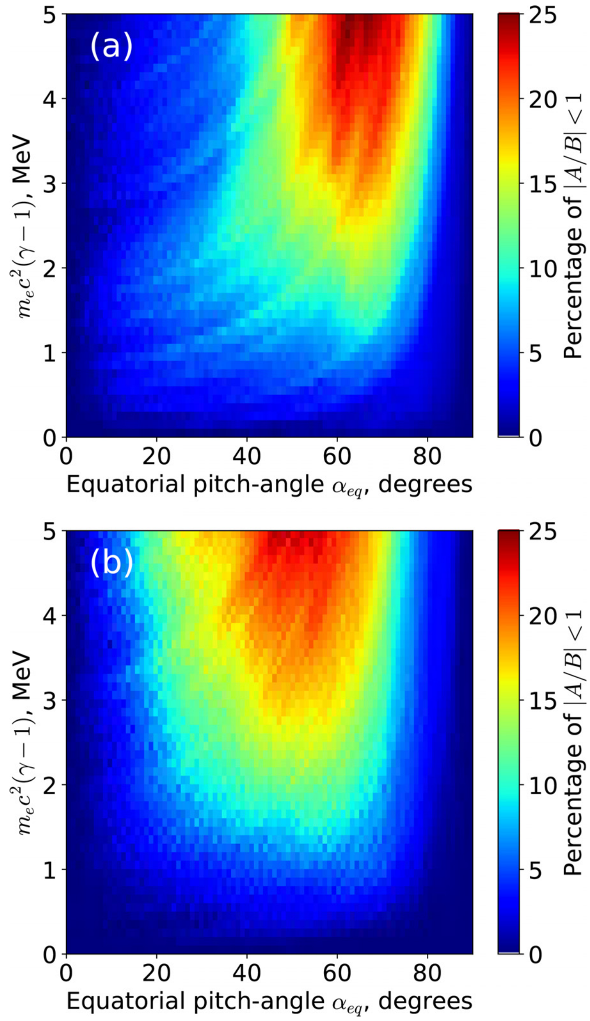

FIG. 6. Percentage of EMIC waves resonating with electrons in the regime of $|A/B| < 1$, i.e., with a finite resonance width. Wave statistics at $L \in [4, 6]$ from Ref. 67 has been used. Panel (a) shows results for H-band EMIC waves in purely proton plasma, and panel (b) shows results for He-band EMIC waves in plasma with 20% of He^+ ions.

and the same inequality means that electrons resonate with EMIC waves nonlinearly[64] with phase trapping and phase bunching effects.[2,27,28,35,36] Nonlinear resonant effects can be suppressed by the wave modulation,[5,25,59,66] but anyway, the resonance broadening effect will lead to a wide range of electron diffusive scattering.[15,31] Therefore, to evaluate the contribution of the resonance broadening to the electron diffusive scattering by EMIC waves, we will investigate the occurrence rate of $|A/B| < 1$ for observed wave and background plasma characteristics. We use EMIC wave statistics from Ref. 67 and evaluate for each event (22s of wave spectrum measurements satisfying the criteria for EMIC waves[13]) the wave intensity $(B_w/B_0)^2$, plasma frequency to gyrofrequency ratio, and L-shell. Then, for a given initial energy and pitch-angle, we find the resonant latitude (under the approximation of a dipole magnetic field) and evaluate $|A/B|$. We examine this for H-band and He-band waves separately, with purely proton plasma for H-band and 20% of He^+ ions for He-band waves (see Ref. 37). Figure 6 shows that about 10% of EMIC waves may support the resonance broadening for > 2MeV, $\alpha_{eq} \in [30, 70]^\circ$ electrons for both wave bands. For $\sim$1 MeV electrons resonating with EMIC around $\alpha_{eq} < 20^\circ$, the percentage of waves supporting the resonance broadening decreases to below 3%. Note that we use 1s averaged wave intensity from the dataset in 67, whereas the instantaneous wave intensity for short wave-packets may be a factor of $\times 10$ larger, which will increase the percentage of electron–EMIC wave interactions with the resonance broadening. Overall, Fig. 6 demonstrates that the resonance broadening effect should extend the pitch-angle range of electron scattering for a significant fraction of observed EMIC waves.

In conclusion, we have quantified the resonance broadening effect for EMIC waves resonating with relativistic electrons. Our model provides the resonance width equation [through the function $f(A/B)$ from Fig. 3] that can be incorporated into diffusion rate calculations. The main result of such generalized diffusion rate equations is the extension of the pitch-angle range of electrons scattered by EMIC waves. This effect can be especially important for $\sim$1 MeV electrons around the minimum resonant energy. Further incorporation of the resonance broadening effect into radiation belt models[18,21,23,39] should improve simulation of relativistic electron losses during geomagnetically active conditions when most intense EMIC waves are observed.

ACKNOWLEDGMENTS

We are grateful to Oliver Allanson for very fruitful discussion of the main results and their presentation.

X.-J.Z. and A.V.A. acknowledge support from the NASA under Grant Nos. 80NSSC20K1270 and NSF 2021749. D.L.V. acknowledges support from the NASA under Grant No. 80NSSC20K1578.

AUTHOR DECLARATIONS

Conflict of Interest

The authors have no conflicts to disclose.

Author Contributions

David Surenovich Tonoian: Formal analysis (lead); Writing – original draft (equal). **Anton Artemyev:** Conceptualization (equal); Methodology (equal); Supervision (equal); Writing – original draft (equal). **Xiaojia Zhang:** Formal analysis (equal); Writing – review and editing (equal). **Mark Shevelev:** Methodology (equal); Supervision (equal). **Dmitri Vainchtein:** Conceptualization (equal); Methodology (equal).

DATA AVAILABILITY

The data that support the findings of this study are openly available in Van Allen Probe data repository at https://emfisis.physics.uiowa.edu/data/index. Data access and processing were done using SPEDAS V4.1, Ref. 6.

REFERENCES

[1] J. M. Albert, "Cyclotron resonance in an inhomogeneous magnetic field," Phys. Fluids B **5**, 2744–2750 (1993).

[2] J. M. Albert and J. Bortnik, "Nonlinear interaction of radiation belt electrons with electromagnetic ion cyclotron waves," Geophys. Res. Lett. **36**, L12110, https://doi.org/10.1029/2009GL038904 (2009).

[3] J. M. Albert, X. Tao, and J. Bortnik, "Aspects of nonlinear wave–particle interactions," in *Dynamics of the Earth's Radiation Belts and Inner Magnetosphere*, edited by D. Summers, I. U. Mann, D. N. Baker, and M. Schulz (American Geophysical Union, 2013).

[4] O. Allanson, E. Thomas, C. E. J. Watt, and T. Neukirch, "Weak turbulence and quasilinear diffusion for relativistic wave-particle interactions via a Markov approach," Front. Phys. **8**, 805699 (2022).

[5] Z. An, Y. Wu, and X. Tao, "Electron dynamics in a chorus wave field generated from particle-in-cell simulations," Geophys. Res. Lett. **49**, e2022GL097778, https://doi.org/10.1029/2022GL097778 (2022).

[6] V. Angelopoulos, P. Cruce, A. Drozdov, E. W. Grimes, N. Hatzigeorgiu, D. A. King, D. Larson, J. W. Lewis, J. M. McTiernan, D. A. Roberts, C. L. Russell, T. Hori, Y. Kasahara, A. Kumamoto, A. Matsuoka, Y. Miyashita, Y. Miyoshi, I. Shinohara, M. Teramoto, J. B. Faden, A. J. Halford, M. McCarthy, R. M. Millan, J. G. Sample, D. M. Smith, L. A. Woodger, A. Masson, A. A. Narock, K. Asamura, T. F. Chang, C. Y. Chiang, Y. Kazama, K. Keika, S. Matsuda, T. Segawa, K. Seki, M. Shoji, S. W. Y. Tam, N. Umemura, B. J. Wang, S. Y. Wang, R. Redmon, J. V. Rodriguez, H. J. Singer, J. Vandegriff, S. Abe, M. Nose, A. Shinbori, Y. M. Tanaka, S. UeNo, L. Andersson, P. Dunn, C. Fowler, J. S. Halekas, T. Hara, Y. Harada, C. O. Lee, R. Lillis, D. L. Mitchell, M. R. Argall, K. Bromund, J. L. Burch, I. J. Cohen, M. Galloy, B. Giles, A. N. Jaynes, O. Le Contel, M. Oka, T. D. Phan, B. M. Walsh, J. Westlake, F. D. Wilder, S. D. Bale, R. Livi, M. Pulupa, P. Whittlesey, A. DeWolfe, B. Harter, E. Lucas, U. Auster, J. W. Bonnell, C. M. Cully, E. Donovan, R. E. Ergun, H. U. Frey, B. Jackel, A. Keiling, H. Korth, J. P. McFadden, Y. Nishimura, F. Plaschke, P. Robert, D. L. Turner, J. M. Weygand, R. M. Candey, R. C. Johnson, T. Kovalick, M. H. Liu, R. E. McGuire, A. Breneman, K. Kersten, and P. Schroeder, "The space physics environment data analysis system (SPEDAS)," Space Sci. Rev. **215**, 9 (2019).

[7] A. V. Artemyev, A. I. Neishtadt, D. L. Vainchtein, A. A. Vasiliev, I. Y. Vasko, and L. M. Zelenyi, "Trapping (capture) into resonance and scattering on resonance: Summary of results for space plasma systems," Commun. Nonlinear Sci. Numer. Simul. **65**, 111–160 (2018).

[8] D. N. Baker, S. G. Kanekal, V. C. Hoxie, S. Batiste, M. Bolton, X. Li, S. R. Elkington, S. Monk, R. Reukauf, S. Steg, J. Westfall, C. Belting, B. Bolton, D. Braun, B. Cervelli, K. Hubbell, M. Kien, S. Knappmiller, S. Wade, B. Lamprecht, K. Stevens, J. Wallace, A. Yehle, H. E. Spence, and R. Friedel, "The relativistic electron-proton telescope (REPT) instrument on board the radiation belt storm probes (RBSP) spacecraft: Characterization of Earth's radiation belt high-energy particle populations," Space Sci. Rev. **179**, 337–381 (2013).

[9] M. F. Bashir, A. Artemyev, X. J. Zhang, and V. Angelopoulos, "Energetic electron precipitation driven by the combined effect of ULF, EMIC, and whistler waves," J. Geophys. Res.: Space Phys. **127**, e2021JA029871, https://doi.org/10.1029/2021JA029871 (2022).

[10] T. F. Bell, "The nonlinear gyroresonance interaction between energetic electrons and coherent VLF waves propagating at an arbitrary angle with respect to the Earth's magnetic field," J. Geophys. Res. **89**, 905–918, https://doi.org/10.1029/JA089iA02p00905 (1984).

[11]L. Bingley, V. Angelopoulos, D. Sibeck, X. Zhang, and A. Halford, "The evolution of a pitch-angle 'bite-out' scattering signature caused by EMIC wave activity: A case study," J. Geophys. Res.: Space Phys. **124**, 5042–5055, https://doi.org/10.1029/2018JA026292 (2019).

[12]L. W. Blum, A. Halford, R. Millan, J. W. Bonnell, J. Goldstein, M. Usanova, M. Engebretson, M. Ohnsted, G. Reeves, H. Singer, M. Clilverd, and X. Li, "Observations of coincident EMIC wave activity and duskside energetic electron precipitation on 18–19 January 2013," Geophys. Res. Lett. **42**, 5727–5735, https://doi.org/10.1002/2015GL065245 (2015).

[13]J. Bortnik, J. W. Cutler, C. Dunson, and T. E. Bleier, "An automatic wave detection algorithm applied to Pc1 pulsations," J. Geophys. Res. **112**, A04204, https://doi.org/10.1029/2006JA011900 (2007).

[14]A. Bruno, L. W. Blum, G. A. de Nolfo, R. Kataoka, S. Torii, A. D. Greeley, S. G. Kanekal, A. W. Ficklin, T. G. Guzik, and S. Nakahira, "EMIC-wave driven electron precipitation observed by CALET on the International Space Station," Geophys. Res. Lett. **49**, e2021GL097529, https://doi.org/10.1029/2021GL097529 (2022).

[15]B. Cai, Y. Wu, and X. Tao, "Effects of nonlinear resonance broadening on interactions between electrons and whistler mode waves," Geophys. Res. Lett. **47**, e2020GL087991, https://doi.org/10.1029/2020GL087991 (2020).

[16]E. Camporeale and G. Zimbardo, "Wave-particle interactions with parallel whistler waves: Nonlinear and time-dependent effects revealed by particle-in-cell simulations," Phys. Plasmas **22**, 092104 (2015).

[17]X. Cao, Y. Y. Shprits, B. Ni, and I. S. Zhelavskaya, "Scattering of ultra-relativistic electrons in the Van Allen radiation belts accounting for hot plasma effects," Sci. Rep. **7**, 17719 (2017).

[18]L. Capannolo, W. Li, Q. Ma, L. Chen, X. C. Shen, H. E. Spence, J. Sample, A. Johnson, M. Shumko, D. M. Klumpar, and R. J. Redmon, "Direct observation of sub-relativistic electron precipitation potentially driven by EMIC waves," Geophys. Res. Lett. **22**, 12711–12721, https://doi.org/10.1029/2019GL084202 (2019).

[19]L. Chen, H. Zhu, and X. Zhang, "Wavenumber analysis of EMIC waves," Geophys. Res. Lett. **46**, 5689–5697, https://doi.org/10.1029/2019GL082686 (2019).

[20]R. E. Denton, L. Ofman, Y. Y. Shprits, J. Bortnik, R. M. Millan, C. J. Rodger, C. L. da Silva, B. N. Rogers, M. K. Hudson, K. Liu, K. Min, A. Glocer, and C. Komar, "Pitch angle scattering of sub-MeV relativistic electrons by electromagnetic ion cyclotron waves," J. Geophys. Res.: Space Phys. **124**, 5610–5626, https://doi.org/10.1029/2018JA026384 (2019).

[21]A. Y. Drozdov, H. J. Allison, Y. Y. Shprits, M. E. Usanova, A. Saikin, and D. Wang, "Depletions of multi-MeV electrons and their association to minima in phase space density," Geophys. Res. Lett. **49**, e2021GL097620, https://doi.org/10.1029/2021GL097620 (2022).

[22]A. Y. Drozdov, N. Aseev, F. Effenberger, D. L. Turner, A. Saikin, and Y. Y. Shprits, "Storm time depletions of multi-MeV radiation belt electrons observed at different pitch angles," J. Geophys. Res.: Space Phys. **124**, 8943–8953, https://doi.org/10.1029/2019JA027332 (2019).

[23]A. Y. Drozdov, Y. Y. Shprits, M. E. Usanova, N. A. Aseev, A. C. Kellerman, and H. Zhu, "EMIC wave parameterization in the long-term VERB code simulation," J. Geophys. Res. **122**, 8488–8501, https://doi.org/10.1002/2017JA024389 (2017).

[24]M. J. Engebretson, J. L. Posch, J. R. Wygant, C. A. Kletzing, M. R. Lessard, C. L. Huang, H. E. Spence, C. W. Smith, H. J. Singer, Y. Omura, R. B. Horne, G. D. Reeves, D. N. Baker, M. Gkioulidou, K. Oksavik, I. R. Mann, T. Raita, and K. Shiokawa, "Van Allen probes, NOAA, GOES, and ground observations of an intense EMIC wave event extending over 12 h in magnetic local time," J. Geophys. Res. **120**, 5465–5488, https://doi.org/10.1002/2015JA021227 (2015).

[25]L. Gan, W. Li, Q. Ma, J. M. Albert, A. V. Artemyev, and J. Bortnik, "Nonlinear interactions between radiation belt electrons and chorus waves: Dependence on wave amplitude modulation," Geophys. Res. Lett. **47**, e2019GL085987, https://doi.org/10.1029/2019GL085987 (2020).

[26]V. S. Grach and A. G. Demekhov, "Resonance interaction of relativistic electrons with ion-cyclotron waves. I. Specific features of the nonlinear interaction regimes," Radiophys. Quantum Electron. **60**, 942–959 (2018).

[27]V. S. Grach and A. G. Demekhov, "Precipitation of relativistic electrons under resonant interaction with electromagnetic ion cyclotron wave packets," J. Geophys. Res.: Space Phys. **125**, e2019JA027358, https://doi.org/10.1029/2019JA027358 (2020).

[28]V. S. Grach, A. G. Demekhov, and A. V. Larchenko, "Resonant interaction of relativistic electrons with realistic electromagnetic ion-cyclotron wave packets," Earth, Planets Space **73**, 129 (2021).

[29]J. C. Green, T. G. Onsager, T. P. O'Brien, and D. N. Baker, "Testing loss mechanisms capable of rapidly depleting relativistic electron flux in the Earth's outer radiation belt," J. Geophys. Res. **109**, A12211, https://doi.org/10.1029/2004JA010579 (2004).

[30]C. W. Jun, C. Yue, J. Bortnik, L. R. Lyons, Y. Nishimura, and C. Kletzing, "EMIC wave properties associated with and without injections in the inner magnetosphere," J. Geophys. Res.: Space Phys. **124**, 2029–2045, https://doi.org/10.1029/2018JA026279 (2019).

[31]H. Karimabadi, D. Krauss-Varban, and T. Terasawa, "Physics of pitch angle scattering and velocity diffusion, 1. Theory," J. Geophys. Res. **97**, 13853–13864, https://doi.org/10.1029/92JA00997 (1992).

[32]C. F. F. Karney, "Stochastic ion heating by a lower hybrid wave," Phys. Fluids **21**, 1584–1599 (1978).

[33]C. F. Kennel and F. Engelmann, "Velocity space diffusion from weak plasma turbulence in a magnetic field," Phys. Fluids **9**, 2377–2388 (1966).

[34]T. Kersten, R. B. Horne, S. A. Glauert, N. P. Meredith, B. J. Fraser, and R. S. Grew, "Electron losses from the radiation belts caused by EMIC waves," J. Geophys. Res. **119**, 8820–8837, https://doi.org/10.1002/2014JA020366 (2014).

[35]Y. Kubota and Y. Omura, "Rapid precipitation of radiation belt electrons induced by EMIC rising tone emissions localized in longitude inside and outside the plasmapause," J. Geophys. Res.: Space Phys. **122**, 293–309, https://doi.org/10.1002/2016JA023267 (2017).

[36]Y. Kubota and Y. Omura, "Nonlinear dynamics of radiation belt electrons interacting with chorus emissions localized in longitude," J. Geophys. Res.: Space Phys. **123**, 4835–4857, https://doi.org/10.1029/2017JA025050 (2018).

[37]J. H. Lee and V. Angelopoulos, "On the presence and properties of cold ions near Earth's equatorial magnetosphere," J. Geophys. Res.: Space Phys. **119**, 1749–1770, https://doi.org/10.1002/2013JA019305 (2014).

[38]L. R. Lyons, R. M. Thorne, and C. F. Kennel, "Pitch-angle diffusion of radiation belt electrons within the plasmasphere," J. Geophys. Res. **77**, 3455–3474, https://doi.org/10.1029/JA077i019p03455 (1972).

[39]Q. Ma, W. Li, R. M. Thorne, B. Ni, C. A. Kletzing, W. S. Kurth, G. B. Hospodarsky, G. D. Reeves, M. G. Henderson, H. E. Spence, D. N. Baker, J. B. Blake, J. F. Fennell, S. G. Claudepierre, and V. Angelopoulos, "Modeling inward diffusion and slow decay of energetic electrons in the Earth's outer radiation belt," Geophys. Res. Lett. **42**, 987–995, https://doi.org/10.1002/2014GL062977 (2015).

[40]D. Mourenas, A. V. Artemyev, Q. Ma, O. V. Agapitov, and W. Li, "Fast dropouts of multi-MeV electrons due to combined effects of EMIC and whistler mode waves," Geophys. Res. Lett. **43**, 4155–4163, https://doi.org/10.1002/2016GL068921 (2016).

[41]A. I. Neishtadt and A. A. Vasiliev, "Destruction of adiabatic invariance at resonances in slow fast Hamiltonian systems," Nucl. Instrum. Methods Phys. Res., Sect. A **561**, 158–165 (2006).

[42]B. Ni, X. Cao, Y. Y. Shprits, D. Summers, X. Gu, S. Fu, and Y. Lou, "Hot plasma effects on the cyclotron-resonant pitch-angle scattering rates of radiation belt electrons due to EMIC waves," Geophys. Res. Lett. **45**, 21–30, https://doi.org/10.1002/2017GL076028 (2018).

[43]B. Ni, X. Cao, Z. Zou, C. Zhou, X. Gu, J. Bortnik, J. Zhang, S. Fu, Z. Zhao, R. Shi, and L. Xie, "Resonant scattering of outer zone relativistic electrons by multiband EMIC waves and resultant electron loss time scales," J. Geophys. Res. **120**, 7357–7373, https://doi.org/10.1002/2015JA021466 (2015a).

[44]B. Ni, Z. Zou, X. Gu, C. Zhou, R. M. Thorne, J. Bortnik, R. Shi, Z. Zhao, D. N. Baker, S. G. Kanekal, H. E. Spence, G. D. Reeves, and X. Li, "Variability of the pitch angle distribution of radiation belt ultrarelativistic electrons during and following intense geomagnetic storms: Van Allen Probes observations," J. Geophys. Res. **120**, 4863–4876, https://doi.org/10.1002/2015JA021065 (2015b).

[45]Y. Omura and Q. Zhao, "Nonlinear pitch angle scattering of relativistic electrons by EMIC waves in the inner magnetosphere," J. Geophys. Res. **117**, A08227, https://doi.org/10.1029/2012JA017943 (2012).

[46]Y. Omura and Q. Zhao, "Relativistic electron microbursts due to nonlinear pitch angle scattering by EMIC triggered emissions," J. Geophys. Res. **118**, 5008–5020, https://doi.org/10.1002/jgra.50477 (2013).

[47]T. O'Neil, "Collisionless damping of nonlinear plasma oscillations," Phys. Fluids **8**, 2255–2262 (1965).

[48]T. G. Onsager, G. Rostoker, H. J. Kim, G. D. Reeves, T. Obara, H. J. Singer, and C. Smithtro, "Radiation belt electron flux dropouts: Local time, radial, and particle-energy dependence," J. Geophys. Res. **107**, 1382, https://doi.org/10.1029/2001JA000187 (2002).

[49]K. G. Orlova and Y. Y. Shprits, "On the bounce-averaging of scattering rates and the calculation of bounce period," Phys. Plasmas **18**, 092904 (2011).

[50]P. J. Palmadesso, "Resonance, particle trapping, and Landau damping in finite amplitude obliquely propagating waves," Phys. Fluids **15**, 2006–2013 (1972).

[51]D. R. Shklyar and H. Matsumoto, "Oblique whistler-mode waves in the inhomogeneous magnetospheric plasma: Resonant interactions with energetic charged particles," Surv. Geophys. **30**, 55–104 (2009).

[52]Y. Y. Shprits, A. Kellerman, N. Aseev, A. Y. Drozdov, and I. Michaelis, "Multi-MeV electron loss in the heart of the radiation belts," Geophys. Res. Lett. **44**, 1204–1209, https://doi.org/10.1002/2016GL072258 (2017).

[53]I. Silin, I. R. Mann, R. D. Sydora, D. Summers, and R. L. Mace, "Warm plasma effects on electromagnetic ion cyclotron wave MeV electron interactions in the magnetosphere," J. Geophys. Res.: Space Phys. **116**, A05215, https://doi.org/10.1029/2010JA016398 (2011).

[54]T. H. Stix, *The Theory of Plasma Waves* (McGraw-Hill, 1962).

[55]Z. Su, H. Zhu, F. Xiao, H. Zheng, C. Shen, Y. Wang, and S. Wang, "Bounce-averaged advection and diffusion coefficients for monochromatic electromagnetic ion cyclotron wave: Comparison between test-particle and quasi-linear models," J. Geophys. Res.: Space Phys. **117**, A09222, https://doi.org/10.1029/2012JA017917 (2012).

[56]D. Summers, "Quasi-linear diffusion coefficients for field-aligned electromagnetic waves with applications to the magnetosphere," J. Geophys. Res. **110**, A08213, https://doi.org/10.1029/2005JA011159 (2005).

[57]D. Summers, B. Ni, and N. P. Meredith, "Timescales for radiation belt electron acceleration and loss due to resonant wave-particle interactions: 1. Theory," J. Geophys. Res. **112**, A04206, https://doi.org/10.1029/2006JA011801 (2007).

[58]D. Summers and R. M. Thorne, "Relativistic electron pitch-angle scattering by electromagnetic ion cyclotron waves during geomagnetic storms," J. Geophys. Res. **108**, 1143, https://doi.org/10.1029/2002JA009489 (2003).

[59]X. Tao, J. Bortnik, J. M. Albert, R. M. Thorne, and W. Li, "The importance of amplitude modulation in nonlinear interactions between electrons and large amplitude whistler waves," J. Atmos. Sol.-Terr. Phys. **99**, 67–72 (2013).

[60]R. M. Thorne and C. F. Kennel, "Relativistic electron precipitation during magnetic storm main phase," J. Geophys. Res. **76**, 4446, https://doi.org/10.1029/JA076i019p04446 (1971).

[61]A. Y. Ukhorskiy, Y. Y. Shprits, B. J. Anderson, K. Takahashi, and R. M. Thorne, "Rapid scattering of radiation belt electrons by storm-time EMIC waves," Geophys. Res. Lett. **37**, L09101, https://doi.org/10.1029/2010GL042906 (2010).

[62]M. E. Usanova, A. Drozdov, K. Orlova, I. R. Mann, Y. Shprits, M. T. Robertson, D. L. Turner, D. K. Milling, A. Kale, D. N. Baker, S. A. Thaller, G. D. Reeves, H. E. Spence, C. Kletzing, and J. Wygant, "Effect of EMIC waves on relativistic and ultrarelativistic electron populations: Ground-based and Van Allen Probes observations," Geophys. Res. Lett. **41**, 1375–1381, https://doi.org/10.1002/2013GL059024 (2014).

[63]B. Wang, Z. Su, Y. Zhang, S. Shi, and G. Wang, "Nonlinear landau resonant scattering of near equatorially mirroring radiation belt electrons by oblique emic waves," Geophys. Res. Lett. **43**, 3628–3636, https://doi.org/10.1002/2016GL068467 (2016).

[64]G. Wang, Z. Su, H. Zheng, Y. Wang, M. Zhang, and S. Wang, "Nonlinear fundamental and harmonic cyclotron resonant scattering of radiation belt ultrarelativistic electrons by oblique monochromatic emic waves," J. Geophys. Res. **122**, 1928–1945, https://doi.org/10.1002/2016JA023451 (2017).

[65]Y. Xu and J. Egedal, "Pitch angle scattering of fast particles by low frequency magnetic fluctuations," Phys. Plasmas **29**, 010701 (2022).

[66]X. J. Zhang, O. Agapitov, A. V. Artemyev, D. Mourenas, V. Angelopoulos, W. S. Kurth, J. W. Bonnell, and G. B. Hospodarsky, "Phase decoherence within intense chorus wave packets constrains the efficiency of nonlinear resonant electron acceleration," Geophys. Res. Lett. **47**, e2020GL089807, https://doi.org/10.1029/2020GL089807 (2020).

[67]X. J. Zhang, W. Li, R. M. Thorne, V. Angelopoulos, J. Bortnik, C. A. Kletzing, W. S. Kurth, and G. B. Hospodarsky, "Statistical distribution of EMIC wave spectra: Observations from Van Allen Probes," Geophys. Res. Lett. **43**, 12348, https://doi.org/10.1002/2016GL071158 (2016).

[68]X. J. Zhang, D. Mourenas, A. V. Artemyev, V. Angelopoulos, and R. M. Thorne, "Contemporaneous EMIC and whistler mode waves: Observations and consequences for MeV electron loss," Geophys. Res. Lett. **44**, 8113–8121, https://doi.org/10.1002/2017GL073886 (2017).

[69]J. P. J. Ross, S. A. Glauert, R. B. Horne, C. E. Watt, N. P. Meredith, and E. E. Woodfield, "A new approach to constructing models of electron diffusion by EMIC waves in the radiation belts," Geophys. Res. Lett. **47**, e88976, https://doi.org/10.1029/2020GL088976 (2020).

[70]J. P. J. Ross, S. A. Glauert, R. B. Horne, C. E. Watt, and N. P. Meredith, "On the variability of EMIC waves and the consequences for the relativistic electron radiation belt population," J. Geophys. Res. (Space Physics) **126**, e29754, https://doi.org/10.1029/2021JA029754 (2021).